Developmental Biology **247,** 390–404 (2002)
doi:10.1006/dbio.2002.0700



# Structure and Expression of Three *Emx* Genes in the Dogfish *Scyliorhinus canicula*: Functional and Evolutionary Implications

**Y. Derobert,* J. L. Plouhinec,* T. Sauka-Spengler,* C. Le Mentec,* B. Baratte,† D. Jaillard,‡ and S. Mazan*,[1]**

**Equipe Développement et Evolution des Vertébrés, ‡Service Commun de Microscopie Electronique, UPRES-A 8080, Université Paris-Sud, 91405 Orsay, France; and †Station Biologique de Roscoff, Place Georges Teissier, 29682 Roscoff, France*

**We report the characterization of three *Emx* genes in a chondrichthyan, the dogfish *Scyliorhinus canicula*. Comparisons of these genes with their osteichthyan counterparts indicate that the gnathostome *Emx* genes belong to three distinct orthology classes, each containing one of the dogfish genes and either the tetrapod *Emx1* genes (*Emx1* class), the osteichthyan *Emx2* genes (*Emx2* class) or the zebrafish *Emx1* gene (*Emx3* class). While the three classes could be retrieved from the pufferfish genome data, no indication of an *Emx3*-related gene in tetrapods could be found in the databases, suggesting that this class may have been lost in this taxon. Expression pattern comparisons of the three dogfish *Emx* genes and their osteichthyan counterparts indicate that not only telencephalic, but also diencephalic *Emx* expression territories are highly conserved among gnathostomes. In particular, all gnathostomes share an early, dynamic phase of *Emx* expression, spanning presumptive dorsal diencephalic territories, which involves *Emx3* in the dogfish, but another orthology class, *Emx2*, in tetrapods. In addition, the dogfish *Emx2* gene shows a highly specific expression domain in the cephalic paraxial mesoderm from the end of gastrulation and throughout neurulation, which suggests a role in the segmentation of the cephalic mesoderm.** 

***Key Words:* *Emx* genes; multigene family; chondrichthyans; dogfish; brain regionalization; cephalic mesoderm.**

## INTRODUCTION

In the last two decades, comparative molecular analyses have provided an increasing body of evidence suggesting that conserved genetic mechanisms may control the early regionalization and patterning of the central nervous system. For instance, an early division into an anterior territory, expressing *Otx*/*otd* genes, and a posterior territory, expressing *Hox* genes, appears highly conserved in triploblastic metazoans, including annelids, insects, and a wide range of deuterostomes (Arendt and Nübler-Jung, 1999). The conservation of additional subdivisions in the brain region has also been proposed, mainly on the basis of comparisons between *Drosophila* and the mouse (Arendt and Nübler-Jung, 1996; Hirth and Reichert, 1999). However, the interpretation of such large-scale comparisons can be controversial, as shown by the example of *empty-spiracles*-related genes. In *Drosophila*, the homeobox *empty-spiracles* (*ems*) gene plays a major role in the development of the brain, and its inactivation results in a gap gene phenotype, characterized by the specific deletion of the two posterior-most neuromeres, the deutocerebrum and the tritocerebrum (Hirth *et al.*, 1995). In the mouse, two *ems*-related genes (called *Emx1* and *Emx2*) have been characterized. Like their *Drosophila* ortholog, both are transcribed in specific neuromeres of the embryonic brain, showing a prominent expression in the dorsal telencephalon, with a sharp posterior limit at the telencephalon–diencephalon boundary. This observation has led to the suggestion that *ems*-related genes may be part of an ancestral genetic network controlling early forebrain regionalization (Simeone *et al.*, 1992a,b). However, functional analyses in mice and comparative analyses in chordates have failed to bring a strong support to this conclusion. First, inactivations of *Emx1* and *Emx2* in mice result in relatively weak brain phenotypes, which substantially differ from the broad deletions observed in *Drosophila*. Only minor defects in the

[1] To whom correspondence should be addressed. Fax: (33-1) 69 15 68 28. E-mail: sylvie.mazan@ibaic.u-psud.fr.

0012-1606/02 $35.00

corpus callosum have been observed in *Emx1*$^{-/-}$ mice, in some, but not all, genetic backgrounds (Qiu *et al.*, 1996). Similarly, *Emx2*$^{-/-}$ mice die at birth due to defects in the urogenital system, another major site of *Emx2* expression, and the brain abnormalities which they display are mainly restricted to medial pallium structures, with a reduction of the hippocampus and the absence of dentate gyrus (Miyamoto *et al.*, 1997; Pellegrini *et al.*, 1997; Yoshida *et al.*, 1997). Second, an *ems*-related gene is present in the two protochordates studied thus far, the ascidian *H. roretzi* and the cephalochordate *Branchiostoma floridae* (Williams and Holland, 2000; Oda and Saiga, 2001). However, expression studies in the former have failed to detect any expression in the central nervous system, transcripts being only present in the epidermis.

A comparative analysis of the expression patterns displayed by *Emx* genes at a shorter evolutionary scale, among vertebrates, can be a first step to understand their functional evolution. Vertebrate *ems*-related genes (termed *Emx*) have been thus far characterized in a wide range of osteichthyans, including the mouse, the zebrafish, *Xenopus*, and the chick (Morita *et al.*, 1995; Pannese *et al.*, 1998; Bell *et al.*, 2001). In all of these species, two paralogous genes, termed *Emx1* and *Emx2*, have been identified. These genes clearly derive from gene duplications having occurred in the vertebrate lineage, even though the orthological relationships among *Emx1* genes remain controversial (Patarnello *et al.*, 1997; Williams and Holland, 2000). They all share a prominent dorsal telencephalic expression domain, but display various additional expression sites in restricted areas of the diencephalon and mesencephalon, or in the developing sense organs. An *Emx* gene, *LjEmx*, has also been recently characterized in the lamprey *Lampetra japonica* (Myojin *et al.*, 2001). It shares a highly specific expression territory in the dorsal telencephalon with its osteichthan counterparts (Murakami *et al.*, 2001), but other expression features substantially differ between the two taxa. For instance, no diencephalic expression territories have been thus far described in the lamprey. *LjEmx* also displays a prominent expression in the mesoderm starting from neurulation stages, an expression domain which has never been reported thus far in osteichthyans (Myojin *et al.*, 2001). In order to gain new insights into the structural and functional evolution of vertebrate *Emx* genes, we have characterized these genes in a shark, the dogfish *Scyliorhinus canicula*, which belongs to the chondrichthyans, a group of early emergence among gnathostomes. These data clearly indicate the presence of three *Emx* orthology classes among gnathostomes and provide new insights into the evolution of their expression patterns among gnathostomes.

## MATERIALS AND METHODS

### *Embryos*

Dogfish eggs were collected from freshly killed *S. canicula* females and kept in oxygenated sea water at 14°C until the desired stages were reached. After carefully opening the egg shell, the embryos were dissected and staged according to Ballard *et al.* (1993).

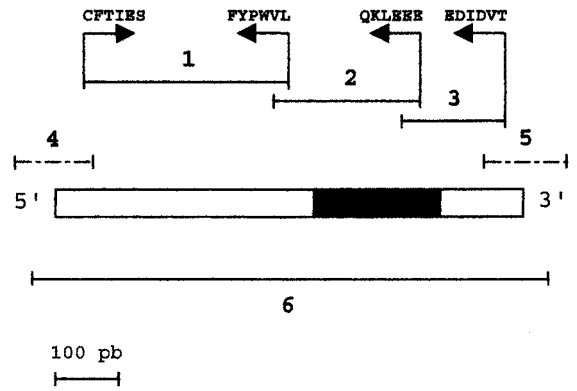


**FIG. 1.** Strategy of amplification of *ScEmx*-coding regions in the dogfish *S. canicula*. The coding region is depicted by a rectangle with the homeodomain in black. Horizontal lines above the coding region delineate partially overlapping cDNA (continuous lines) or genomic (dotted lines) fragments, which were successively amplified for each *ScEmx* gene identified. These fragments are numbered from 1 to 5, following their order of amplification. The location and sequence of conserved protein motifs which were used to choose degenerate amplification primers are indicated, with an arrow showing the primer 5′–3′ orientation. Fragment 6 (horizontal line below the coding sequence) was amplified as a control in a single RT-PCR step.

### *cDNA Amplification and Sequence Analysis*

The strategy used to characterize *Emx* homologs in the dogfish *S. canicula* consisted in the successive amplification and sequencing of five partially overlapping DNA segments numbered from 1 to 5, following their order of amplification (Fig. 1). Fragments 1, 2, and 3 were amplified from dogfish embryonic cDNA (stage 21) by using a degenerate RT-PCR approach. Fragment 1 was first amplified by a seminested PCR, using as 5′ primer, 5′-TGYTTYACNATHGARTC-3′, and as 3′ primers, 5′-YTGRAANCKRTGNCCNA-3′ and 5′-ATNARCCANGGRTARAA-3′. These three primers respectively correspond to the CFTIES, FYPWVL, and FYPWLI motifs conserved among osteichthyan *Emx* genes (cycling conditions: 95°C, 1 min; 45°C, 1 min; 72°C, 1 min; 40 cycles). Fragments 2 and 3 were then successively amplified by using nested 5′ primers located in PCR fragment 1 and specific for each *Emx* gene identified, and degenerate 3′ primers corresponding to the QKLEEE and (E/D)(E/D)IDVT protein motifs (respectively, 5′-TCYTCYTCNARYTTYTG-3′ and 5′-GTNACRTCDATNTCYTC-3′; cycling conditions: 95°C, 1 min; 45–50°C, 1 min; 72°C, 1 min, 40 cycles). Genomic DNA fragments encoding the N-terminal and C-terminal parts of each Emx protein identified (fragments 4 and 5 in Fig. 1) were obtained by inverse PCR, starting from digested and religated adult liver genomic DNA, and using specific primers chosen in the neighboring sequenced fragments (fragments 1 and 3). As a control, a cDNA fragment spanning the full-length coding region was amplified for each gene identified, in a single RT-PCR step, using specific primers located upstream of the initiation codon and

downstream from the termination codon (fragment 6 in Fig. 1). Amplified fragments were subcloned and sequenced by using standard protocols. In each case, nucleotide sequences were deduced from the consensus sequence of at least three independent clones. The three dogfish *Emx* sequences identified were submitted to GenBank under the following Accession Nos.: AF306635, AF306636, and AF306637.

### *Phylogenetic Analysis and Database Search*

The following Emx protein sequences were retrieved from the GenBank database or from the following references: *Mus musculus* Emx1 and Emx2, *Homo sapiens* Emx1 and Emx2 (Patarnello *et al.*, 1997), *Gallus gallus* Emx1 and Emx2 (Bell *et al.*, 2001), *Xenopus laevis* Emx1 and Emx2 (Pannese *et al.*, 1998), *Danio rerio* Emx1 (D32214) and Emx2 (D32215), *Oryzias latipes* Emx1 (AJ250402) and Emx2 (AJ132403), *L. japonica Emx* (AB048759), and *B. floridae* EmxA (AF261146). Similarities to Emx coding sequences were found in scaffolds retrieved from http://fugu.hgmp.mrc.ac.uk/fugu-bin/clonesearch, with the following Accession Nos.: scaffold 6997 (FT:T006997), scaffold 12441 (FT:T012438), scaffold 12231 (FT: T012228), scaffold 2114 (FT:T002114), and scaffold 2099 (FT: T002099). Human Emx1 and Emx2 sequences, which are almost identical to their mouse orthologs and the chick partial Emx1 sequence were excluded from the phylogenetic analysis. The sequences were aligned by using the ED program of the MUST package (Philippe, 1993). Similarities to Emx protein sequences were searched for in the genomic and EST sequences available from human, mouse, pufferfish, and zebrafish (NCBI human and mouse genomic BLAST pages, NCBI EST database, and Fugu Genome Consortium BLAST page) by using the tblastn algorithm (Altschul *et al.*, 1997) with *X. laevis* and *D. rerio* Emx1 and Emx2 protein sequences as inputs. Sequences displaying strong similarities were retrieved and further analyzed. Phylogenetic analyses were performed by using neighbor-joining (NJ), maximum-parsimony (MP), and maximum likelihood analyses (ML). For the NJ analyses, distance matrixes were calculated according to Rzhetsky and Nei (1994) with parameter alpha set to 0.5 according to the ML estimate, and trees were constructed by using the NJ program of the MUST package. MP analyses were performed by using the branch and bound algorithm available in PAUP version 3.1.1 (Swofford, 1993), and ML was conducted by using PROTML version 2.3 (Adachi and Hasegawa, 1996): the best ML tree was chosen among 2000 trees constructed by using the quick-add OTUs method with the JTT-f model of amino acid substitution. Confidence in each node was assessed by 1000 bootstrap replicates in NJ and MP analyses and by the RELL method (Kishino *et al.*, 1990) on the 2000-ml trees constructed.

### *Whole-Mount Hybridization of Dogfish Embryos*

Digoxigenin 11-UTP-labeled antisense RNA probes were transcribed in the presence of T7 RNA polymerase from linearized pTZ19R recombinants containing the whole coding region of each gene identified (fragment 6). Whole-mount hybridizations of dogfish embryos were performed according to standard protocols (Xu and Wilkinson, 1993). No cross-hybridization between the paralogous genes was observed under these conditions. After hybridization, embryos were transferred to 75% glycerol/PBT (PBT: phosphate-buffered saline, 0.1% Tween 20), and photographed or processed for sections.

### *Histological Sections*

Following whole-mount hybridization, embryos were postfixed in 4% paraformaldehyde/PBT (4°C, 12 h), rinsed in PBS, equilibrated in 15% sucrose (4°C, overnight), embedded in 15% sucrose, 20% gelatine (37°C, overnight), frozen in liquid nitrogen, and mounted in O.C.T. embedding compound (Miles Elkhart) for cryostat sections. Then, 20-$\mu$m sections were cut and mounted onto gelatinized slides. The slides were counterstained by using Nuclear Fast Red (Vector Laboratories, Burlingame, CA), dehydrated, mounted in Eukitt (O. Kindler GmbH, Freiburg, Germany), and photographed by using Nomarski optics.

## RESULTS

### *Identification of Three Emx Genes in the Dogfish S. canicula*

To identify *empty-spiracles*-related genes in the dogfish *S. canicula*, we used a degenerate PCR-based strategy, taking advantage of the high phylogenetic conservation of protein motifs present in all osteichthyan Emx proteins (Fig. 1; see Materials and Methods). This strategy led to the characterization of three distinct cDNA fragments, containing open reading frames encoding proteins of 232, 234, and 246 amino acids in length, respectively. The three genes thus identified can be unambiguously assigned to the *ems* class, as shown by their comparison with *Drosophila ems*. First, their deduced amino acid sequences contain a homeodomain which displays a high similarity to the one of *ems* (12–13 differences between ems and each of the three dogfish sequences). This similarity extends to two residues located immediately upstream from the homeobox (RK) and three residues immediately downstream (KEE or EEE in the

**FIG. 2.** Comparison of vertebrate and *Amphioxus* Emx protein sequences. (A) Amino acid sequence alignments. Gaps introduced into the alignment to maximize sequence similarity are shown as asterisks; a dot indicates an amino acid identity. Protein sequences showing a similarity with *Drosophila* ems are overlined with a thick bar; the homeodomain is boxed. Residues selectively conserved in each of the three gnathostome *Emx* orthology classes are shaded in red (class 1), blue (class 2), and yellow (class 3). (B, C) Best ML trees showing the phylogenetic relationships among gnathostome (B) and vertebrate (C) Emx protein sequences. (B) is an unrooted tree; (C) was rooted by using the *Amphioxus* EmxA sequence. Boxed numbers at the nodes indicate bootstrap values supporting the corresponding group (ML, NJ, and MP bootstraps shown in the first, second, and third lines, respectively). *Bf, Branchiostoma floridae*; *Dr, Danio rerio*; *Gg, Gallus gallus*; *Hs, Homo sapiens*; *Mm, Mus musculus*; *Sc, Scyliorhinus canicula*; *Xl, Xenopus laevis*.

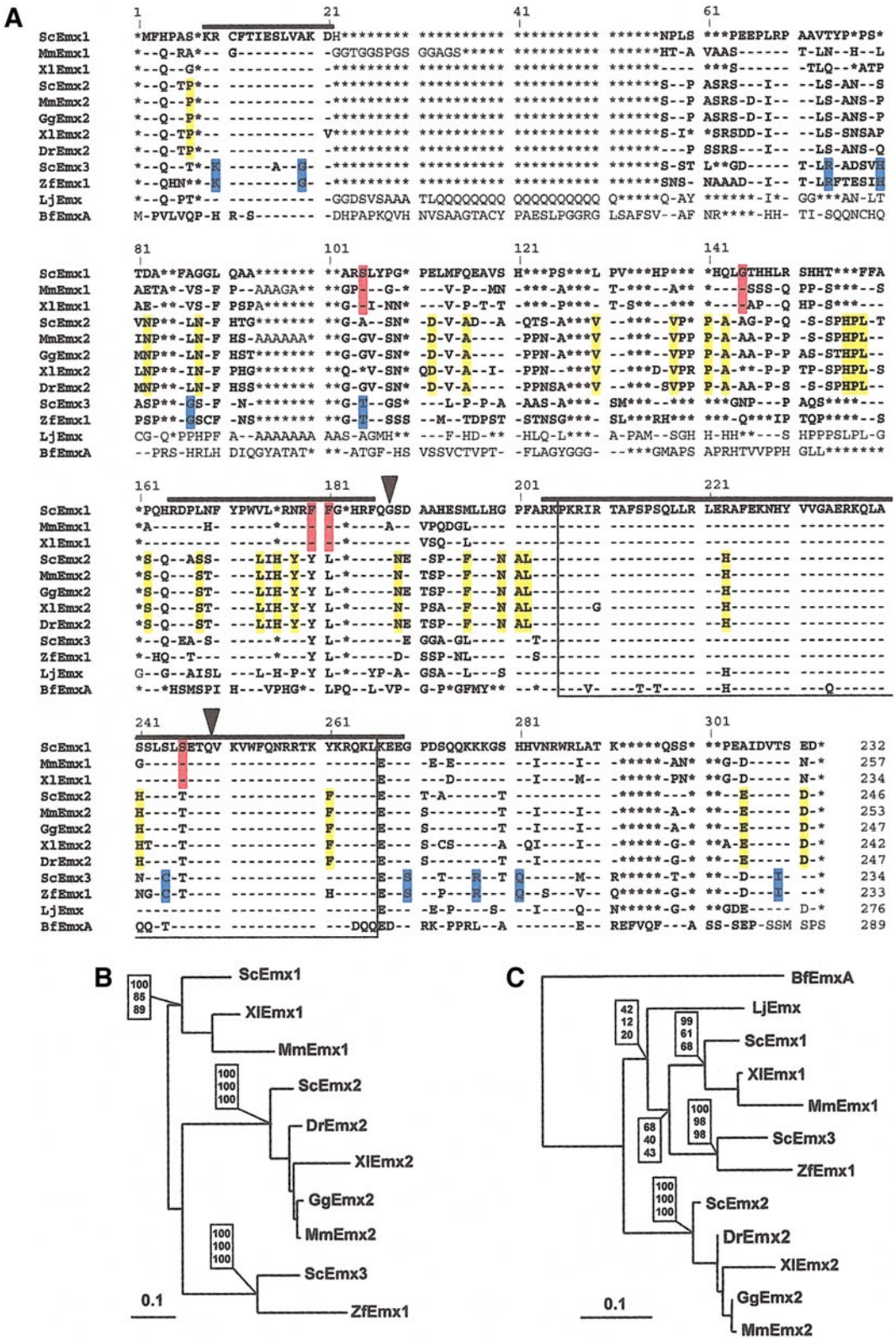

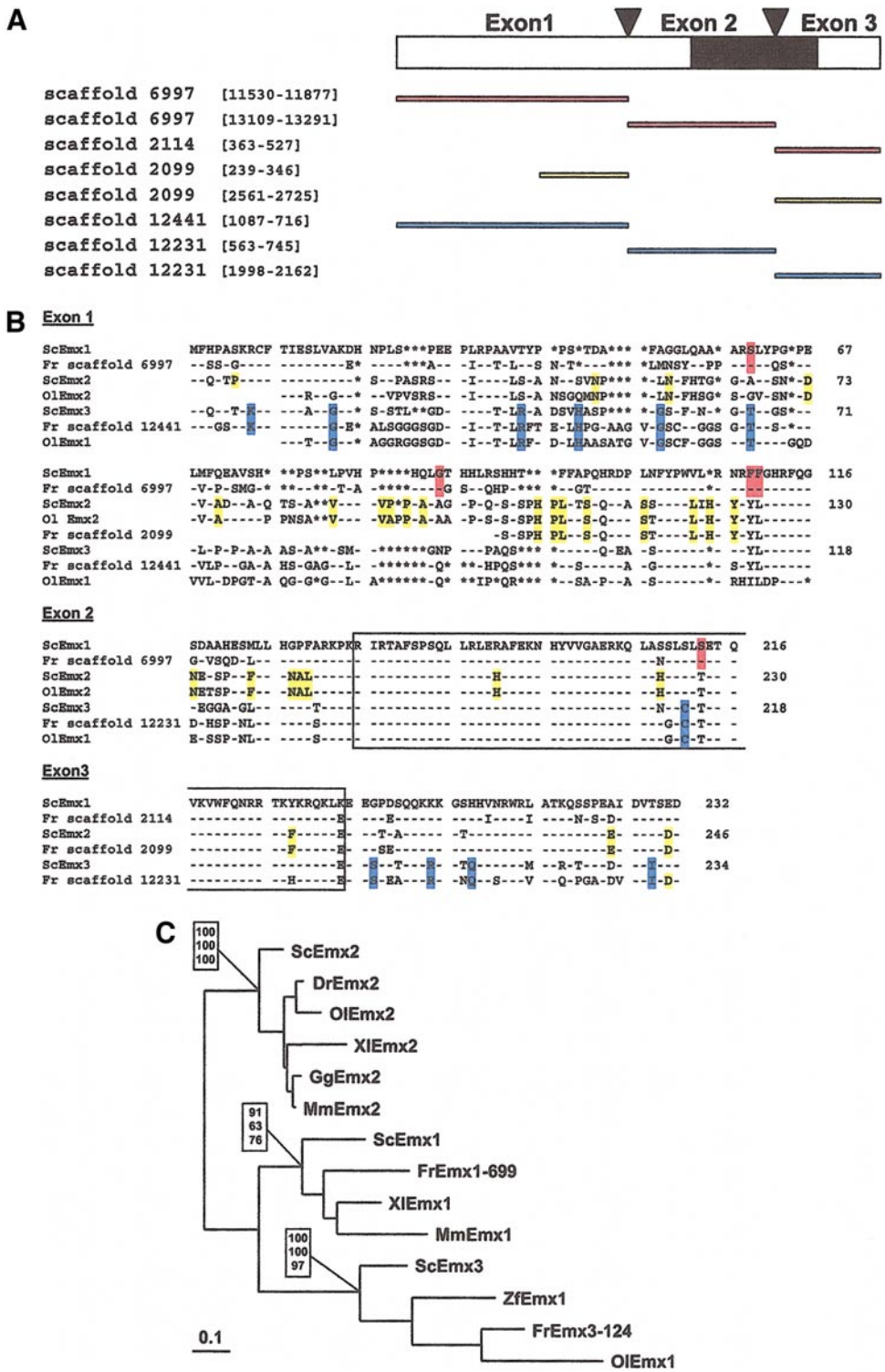


**FIG. 3.** *Emx*-related coding sequences in *F. rubripes*. (A) Scheme showing the position in the coding region of the similarities found in *F. rubripes*. The exon–intron organization of vertebrate Emx-coding sequences is shown in the upper line; a black box indicates the homeodomain, and arrowheads indicate intron–exon junctions. Horizontal bars delimit the region of similarity found in each sequence scaffold relative to the coding sequence. Emx1, Emx2, and Emx3-related sequences are shown in red, yellow, and blue, respectively. Numbers between brackets indicate the position of the similarity in the nucleotide sequence of each scaffold. (B) Alignment of the deduced

dogfish sequences, EEE in ems). Outside the homeodomain, short protein motifs are also conserved, at identical positions, between ems and the dogfish sequences. Like their *Drosophila* orthologue, the three dogfish protein sequences display the 13-amino acid motif $KX_2FXIEX_2VX_2D$ close to their N-terminal end (positions 9–21 in Fig. 2A), and the $RDX_4YPWX_8HRF$ sequence at a short distance upstream of the homeodomain (positions 165–186 in Fig. 2A). The assignment of the three genes identified in *S. canicula* to the vertebrate *Emx* family is also strongly supported by the comparison of their deduced amino acid sequences with those of mouse, human, chick, *Xenopus*, and zebrafish Emx sequences. All three dogfish Emx sequences can be unambiguously aligned with their osteichthyan Emx1 and Emx2 counterparts over the major part of the molecule (bold characters in Fig. 2A), showing a high level of conservation among gnathostome Emx proteins (106 invariant residues out of 250 confidently aligned sites).

### *Phylogenetic Analysis*

In order to investigate orthology relationships between the three dogfish *Emx* genes and the *Emx1* and *Emx2* genes identified in osteichthyans, we performed a first phylogenetic analysis using neighbor-joining (NJ), maximum-parsimony (MP), and maximum likelihood (ML) algorithms (Fig. 2B). The whole protein sequence was taken into account in this analysis, except for two segments, which correspond to broad insertions either in the lamprey and *Amphioxus*, or mammalian sequences (positions 22–56 and 94–102 in Fig. 2A). All three reconstruction methods led to identical tree topologies (Fig. 2B). In all cases, three distinct classes can be identified, each containing a single dogfish and at least one osteichthyan Emx sequence. As expected, the four Emx2 sequences characterized in osteichthyans (MmEmx2, GgEmx2, XlEmx2, and DrEmx2) cluster within a single class (class 2), together with one of the dogfish sequences, thereafter termed ScEmx2. By contrast, a partition of osteichthyan Emx1 sequences into two distinct classes is observed. One of them (class 1) contains the mouse and *Xenopus* Emx1 sequences together with a second dogfish Emx form (which was termed ScEmx1). The zebrafish Emx1 sequence does not emerge within this class but appears closely related to the third dogfish sequence (termed ScEmx3), thus defining a third class (class 3). The partition of the gnathostome *Emx* genes into these three classes is supported by high bootstrap values whatever the reconstruction method used (Fig. 2B). In addition, inside each class, the branching orders of the paralogous genes are identical in the tree reconstruction methods used, and consistent with the gnathostome phylogeny, *ScEmx1* and *ScEmx2* displaying basal positions among gnathostome *Emx1*- and *Emx2*-related genes.

In order to study the relationships of the lamprey *LjEmx* and *Amphioxus EmxA* genes with their gnathostome counterparts, we performed a second analysis including these sequences (Fig. 2C). The alignment segments used in this analysis were restricted to positions 2–21 and 162–312 (Fig. 2A), due to the extensive divergence of the lamprey and *Amphioxus* sequences with their gnathostome counterparts outside these regions. Whatever the reconstruction method used, the monophyly of each of the three gnathostome *Emx* classes is recovered with good statistical supports in this analysis (Fig. 2C). In contrast, the order of emergence of the three classes and the relative position of the lamprey gene were found to vary depending on the reconstruction method used (data not shown) and could not be confidently resolved.

### *Database Search of Novel Osteichthyan Emx1-, Emx2-, and Emx3-Related Sequences*

In order to investigate the presence of representatives of the *Emx3* class in sarcopterygians and of the *Emx1* class in actinopterygians, we performed systematic searches for *Emx*-related sequences in the sequence databases currently available for human, mouse, and zebrafish (http://www.ncbi.nlm.nih.gov/BLAST/), and for the pufferfish *Fugu rubripes* (http://fugu.hgmp.mrc.ac.uk/blast/). While both *Emx1* and *Emx2* sequences could be readily retrieved from mouse ESTs and the available human genome data, no indication of a third, *Emx3*-related gene could be obtained in these species. Similarly, no other sequence than those encoding ZfEmx1 and ZfEmx2 could be found in the zebrafish sequence data. In contrast, a strong evidence for the presence of three *Emx* genes was obtained from the pufferfish genomic sequence. In this species, five distinct sequence scaffolds (scaffolds 6997, 2114, 2099, 12441, and 12231) containing a total of eight segments of similarity to *Emx* coding sequences were retrieved from the raw sequence database (Fig. 3A). In most cases, the similarities end accurately at previously reported intron–exon junctions (Figs. 3A and 3B), confirming the conservation of intron positions in chordates (Williams and Holland, 2000). The only exception concerns nucleotides [239–346] in scaffold 2099, whose deduced amino acid sequence shows a very strong similarity to part of the gnathostome Emx2 sequence encoded by the first exon (positions 170–232 in Fig. 2A). However, this similarity is abruptly interrupted upstream of position 105. We could not detect any intron

amino acid of *F. rubripes* Emx-related sequences with *S. canicula* and *O. latipes* Emx sequences. (C) Best ML tree showing the relationships of the Emx sequences retrieved from the pufferfish genome database with other gnathostome Emx sequences. Only sequences encoded in the first exon were taken into account. Same abbreviations as in Fig. 2. *Fr, Fugu rubripes*; *Ol, Oryzias latipes*.

acceptor site or candidate initiation methionine in the vicinity of this truncation, and its biological significance remains unclear. Similarities to exon 2 could not be detected in this scaffold, but may be present in undetermined sequences lying between positions 964 and 1387.

To study the relationships of the Emx sequences deduced from the *F. rubripes* genome with their gnathostome counterparts, we included their deduced amino acid sequences in the alignment shown in Fig. 2A, together with two medaka partial sequences retrieved from GenBank as *OlEmx1* and *OlEmx2* (Fig. 3B; and data not shown). A third phylogenetic analysis including these sequences was performed by using ML, NJ, and MP algorithms (Fig. 3C). This analysis was restricted to the protein sequences encoded by the first exon, which vary substantially among the three Emx classes. The *Fugu* Emx sequences contained in scaffold 2099, which display a truncation in this region, were excluded from this comparison. The resulting phylogenetic tree confirms the partition of the gnathostome Emx sequences into three classes, each containing one of the dogfish sequences and supported by high bootstrap values (Fig. 3C). Whatever the reconstruction method used, the *Fugu* amino acid sequences deduced from scaffolds 6997 and 12441 emerge within the Emx1 and Emx3 classes, respectively. As to the partial Emx sequences identified in scaffold 2099, they are almost identical to the zebrafish and dogfish Emx2 sequences, which supports their assignment to the Emx2 class (Fig. 3B).

The partition of the gnathostome Emx sequences into three distinct classes is further substantiated by the sharing of residues, which appear selectively conserved within each class (shaded in Figs. 2A and 3B). Such distinctive features are observed in relatively variable parts of the molecule, but also in the homeodomain (with three Emx2-specific residues: positions 223, 241, 261; one Emx1-specific residue: position 246; and one Emx3-specific residue: position 244), or in the close vicinity of motifs conserved in *Drosophila* (with five Emx2-specific residues: positions 162, 168, 174, 176, and 178; and two Emx1-specific residues: positions 180 and 181).

## *Expression of ScEmx2 and ScEmx3 during Gastrulation and Neurulation (Stages 13–17)*

***ScEmx1.*** No expression of *ScEmx1* was detectable in *S. canicula* embryos until stage 19.

***ScEmx2.*** *ScEmx2* transcripts were first observed in gastrulating embryos at stage 13. At this stage, *ScEmx2* displays two longitudinal expression domains, symmetrically located on each side of the embryonic axis in its anterior half (Fig. 4A). This expression domain intensifies and its boundaries become more sharply defined at stage 14, when the cephalic enlargement becomes visible (Fig. 4B): at this stage, the hybridization signal is restricted to the cephalic enlargement at a prechordal level of the anterior–posterior axis. Transverse sections show that this *ScEmx2* expression is confined to the lateral mesoderm, being clearly excluded from the axial mesoderm which forms a continuous layer with the adjacent ectoderm and endoderm layers (Figs. 4E and 4H). At stage 17 (neural tube closure), this mesodermal expression is present in the epithelial layer lining the first head coelomic cavity (mandibular cavity), which becomes visible on each side of the embryonic head, with a higher signal intensity in its lateral parts (Figs. 5A and 5C). A hybridization signal in the cephalic mesoderm, located rostrally to the first pharyngeal pouch, is still visible at stage 19 but faints afterwards (Fig. 6A). The signal which is observed at later stages in the head mesenchyme, on each side of the telencephalon and diencephalon (Figs. 7F and 7G) clearly corresponds to a distinct phase of expression. No expression could be detected in the ectoderm until stage 19.

***ScEmx3.*** *ScEmx3* expression was first detected at stage 14. At this stage, a strong hybridization signal appears as two symmetrical lateral stripes lining the anterior border of the head enlargement (Fig. 4C). As shown by transverse sections (Fig. 4F), this signal is restricted to the neural plate, with a sharp lateral boundary at the border between the presumptive neural ectoderm and skin ectoderm. Transcripts are also present in the presumptive skin ectoderm, but at more posterior levels (Figs. 4C and 4I). At later stages, the anterior domains of expression fuse dorsally upon neural tube closure, resulting in a broad dorsal expression domain in the anteriormost part of the neural tube (stage 17; Figs. 5B and 5D). A faint expression in the first pharyngeal pouch is also first observed at stage 17 (Fig. 5B).

## *ScEmx1, ScEmx2, and ScEmx3 Expression in the Embryonic Brain (Stages 19–22; 2.5-cm Embryos)*

***ScEmx1.*** *ScEmx1* transcription was first detectable at low levels in the developing brain at stage 19 (data not shown). During stages 21–22, a faint hybridization signal was observed dorsally, in the caudal part of the telencephalon (Fig. 7A). As shown by sagittal sections, its posterior border of expression is located immediately anterior to the velum transverse, which corresponds dorsally to the dorsal telencephalon–diencephalon boundary (Fig. 7M). Expression declines dorsally, being almost undetectable along the dorsal midline. In 2.5-cm embryos, transcripts display a widely spread distribution, spanning the dorsal telencephalon, the infundibulum, and the dorsal mesencephalon. However, they remain excluded from the dorsal diencephalon (Fig. 8A).

***ScEmx2.*** *ScEmx2* transcription in the embryonic brain was first detected at stage 19, in the ventral half of the prosencephalon, posterior to the optic evagination (Figs. 6A–6C). This ventral expression domain persists at stage 22, with transcripts present in the ventral part of the diencephalon, posterior to the optic stalk, but excluded from the floor plate and adjacent cells (Fig. 7H). At this stage, another domain of expression is observed in the caudal part of the dorsal telencephalon. This expression domain is very similar to the one displayed by *ScEmx1*,

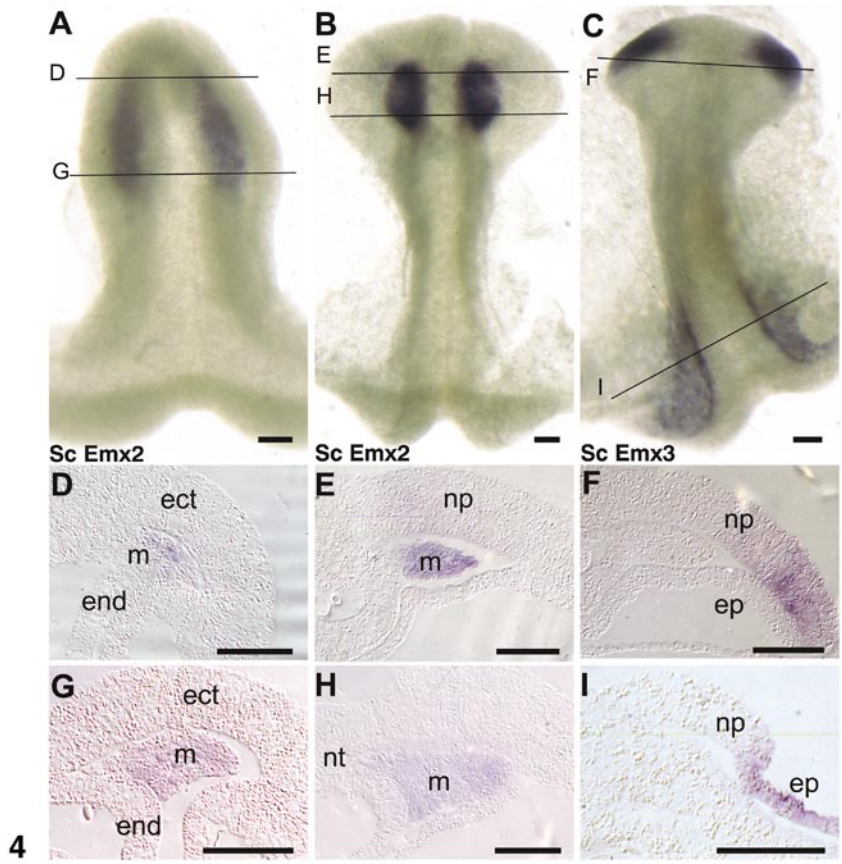


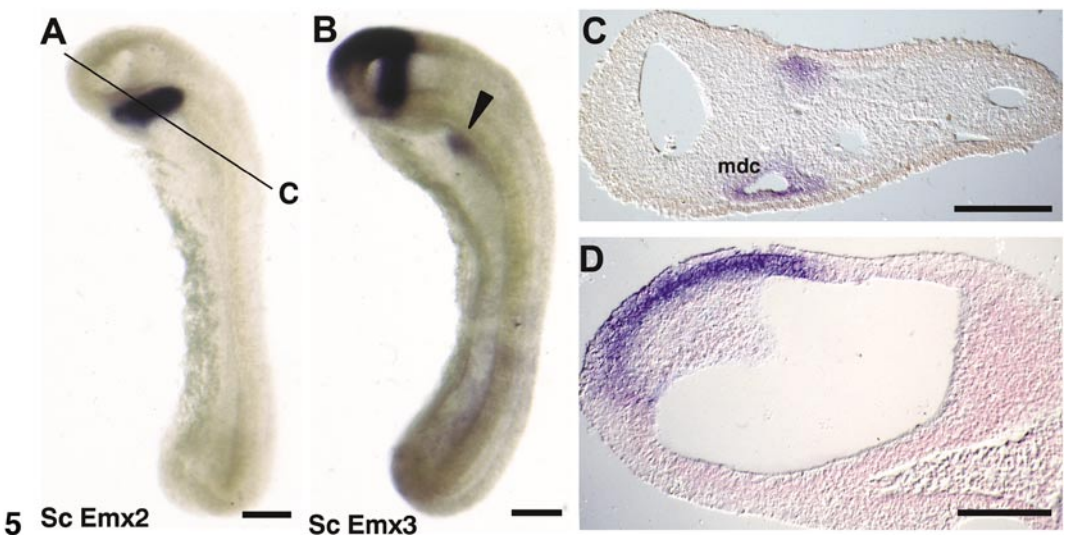


**FIG. 4.** Expression of *ScEmx2* and *ScEmx3* during gastrulation and the beginning of neurulation. (A–C) Dorsal views of stage 13 (A) or stage 14 (B, C) *S. canicula* embryos, after whole-mount hybridization using *ScEmx2* (A, B) or *ScEmx3* (C) antisense RNA probes. Anterior is to the top. (D–I) Transverse half-sections of the embryos shown in (A–C) respectively. Medial is to the left. Thin lines in (A–C) indicate the level of the sections. ect, ectoderm; m, mesoderm; end, endoderm; np, neural plate; ep, presumptive epidermis; nt, notochord.

**FIG. 5.** Expression of *ScEmx2* and *ScEmx3* stage 17 *S. canicula* embryos. (A, B) Lateral views (anterior to the top) of stage 17 embryos after ISH using *ScEmx2* (A) and *ScEmx3* (B) probes. (C, D) Frontal (C) and sagittal (D) sections of the embryos shown in (A) and (B), respectively (anterior to the left). A thin line in (A) indicates the plane of the section shown in (C). A black arrowhead indicates *ScEmx3* expression in the first branchial pouch. mdc, mandibular cavity.


**FIG. 6.** Expression of *ScEmx2* (A–C) and *ScEmx3* (D–G) in stage 19 *S. canicula* embryos. (A, D) Lateral views after whole-mount hybridization. Anterior is to the left. (B, E) Parasagittal sections of the head region. (C, F, G) Transverse sections. The planes of sections are indicated in (A) for the section shown in (C), and in (D) for the sections shown in (F) and (G). The star in (A) indicates a signal in the urogenital system. Open and black arrows point, respectively, to *ScEmx2*-positive signals in the cephalic mesoderm and *ScEmx3*-positive signals in the first and second branchial pouches.

albeit a significantly higher signal intensity was reproducibly observed (Figs. 7E and 7G). At later stages, in 2.5-cm embryos, prominent signals are present in the posterior infundibulum and the dorsal telencephalon with a sharp posterior border at the telencephalon–diencephalon boundary (Fig. 8B). In the telencephalon, the transcripts are excluded from the dorsal midline. A faint and diffuse labeling is also present in the ventral mesencephalon. No transcripts could be detected in the dorsal diencephalon.

***ScEmx3.*** The boundaries of *ScEmx3* expression domain in the anterior part of the neural tube become sharply defined at stage 19 (Figs. 6D–6G). At this stage, *ScEmx3* displays a broad expression domain, extending over the whole dorsal prosencephalon, with a sharp posterior border immediately anterior to the prosencephalon–mesencephalon boundary. Dorsally, a transverse line of expression at the mesencephalon–metencephalon limit can also be observed (Fig. 6D). Both of these expression domains persist during stages 21 and 22 (Fig. 7I). At these stages, *ScEmx3* expression domain in the forebrain is mainly restricted to the dorsal telencephalon but clearly extends dorsally beyond the velum transverse, into diencephalic territories (Figs. 7J–7L and 7O). However, in the absence of morphological landmarks, its boundaries remain difficult to define more precisely. In 2.5-cm embryos, *ScEmx3* shows a prominent expression spanning the telencephalic evaginations and the dorsal midline. At this stage, the signal is completely excluded from more posterior, diencephalic areas (Fig. 8C).

### *Other Sites of Expression*

*ScEmx* genes are also transcribed in other parts of stage 22 embryos, including the otic and olfactory placodes, the pharyngeal arches, and the primordium of the urogenital system. All three *ScEmx* genes are expressed in the olfactory placodes, albeit with nonsuperimposable expression domains. While *ScEmx1* and *ScEmx2* display relatively faint signals, confined to a restricted area located to the middle of the epithelium thickening (Figs. 7A, 7B, 7E, and 7F), *ScEmx3* domain of expression in the olfactory placodes is much broader, extending dorsally into the epidermis, up to the midline (Figs. 7I and 7J). In the otocyst, only *ScEmx2* is transcribed, with a signal restricted to the mediodorsal quadrant. All four anterior pharyngeal arches also express different combinations of *ScEmx* genes at stage 22. *ScEmx1* transcripts remain undetectable until stage 22. At this stage, they are restricted to a posterior ectodermal region, which is located halfway along the proximodistal axis (Fig. 7A; sections not shown). *ScEmx2* and *ScEmx3* expressions in the pharyngeal arches appear earlier, from stage 19 on. At stage 22, *ScEmx2* expression domain only concerns a restricted mesodermal area of the mandibular and hyoid arches, while *ScEmx3* expression is detected in the whole ectoderm of all four visceral arches (Figs. 7E and 7I; sections not shown). Finally, all three genes are expressed in the urogenital system of stage 22 embryos, with a very low signal intensity for *ScEmx3*.

## DISCUSSION

### *Three Orthology Classes among Gnathostome Emx Genes*

The monophyly of osteichthyan *Emx2* genes has been undisputed thus far, but less clear results have been obtained concerning *Emx1* genes in previous phylogenetic

analyses (Patarnello *et al.*, 1997; Williams and Holland, 2000). While the tetrapod *Emx1* genes were always found clustered in a single clade with high support values, the relative position of the zebrafish *Emx1* gene could not be confidently resolved. These ambiguous results led to the suggestion that either this gene had undergone a particularly high rate of evolution in actinopterygians, or it was a member of another class, thus far unidentified in sarcopterygians. The comparison of the three Emx sequences characterized in *S. canicula* with their osteichthyan counterparts provides a strong support in favor of the latter hypothesis. Whatever the method and the parameters used in the phylogenetic analysis, the gnathostome *Emx* genes appear partitioned into three monophyletic groups, each containing one of the three dogfish sequences, and either the sarcopterygian Emx1 (*Emx1* class), the osteichthyan Emx2 (*Emx2* class), or the zebrafish (and medaka) Emx1 sequences (*Emx3* class). We conclude from these results that three *Emx* genes were present in the lineage of gnathostomes prior to their radiation and that the three groups identified in our analysis derive from these ancestral genes. The *Emx1* genes isolated in the zebrafish (or medaka) and in the tetrapods therefore belong to distinct orthology classes.

As shown by the pufferfish genome analysis, all three orthology classes were clearly present in the last common ancestor of teleosts and it will be of great interest to investigate the presence of an *Emx1*-related gene in the zebrafish. In sarcopterygians, the presence of an *Emx3*-related gene remains an unanswered question. The presence of an additional *Emx*-related gene, which could compensate for some of the functions of its paralogs, could account for the relatively weak $Emx1^{-/-}$ and $Emx2^{-/-}$ phenotypes observed in mice. However, while both *Emx1* and *Emx2* coding sequences could be readily retrieved from mouse ESTs and the available human genome data, no indication of a third, *Emx3*-related gene could be obtained in these species. We therefore favor the hypothesis that *Emx3*-related genes have been lost during the evolution of sarcopterygians, prior to the mammalian radiation.

## *Both Telencephalic and Diencephalic Emx Expression Sites Are Conserved among All Gnathostomes*

***Dorsal telencephalon.*** During early organogenesis, all osteichthyan *Emx* genes share broad dorsal expression domains in the telencephalon, showing sharp posterior borders at the telencephalon–diencephalon boundary (Simeone *et al.*, 1992a,b; Pannese *et al.*, 1998; Bell *et al.*, 2001; Morita *et al.*, 1995). Similarly, when the major subdivisions of the lamprey brain become visible (stage 26), the *LjEmx* gene identified in *L. japonica* appears restricted to a dorsal subdomain of the telencephalon. These data have suggested that *Emx* genes could be part of a vertebrate ancestral genetic network, which controls the early regionalization of the telencephalon and is highly conserved in this taxon (Murakami *et al.*, 2001). Our analysis of *Emx* genes in a chondrichthyan supports this conclusion. Like their vertebrate counterparts, the three dogfish *Emx* genes are transcribed in broad domains of the dorsal telencephalon with a sharp posterior border at the telencephalon–diencephalon boundary when the cerebral vesicles become visible. The high conservation of this *Emx* expression border in vertebrates is consistent with an involvement of *Emx* genes in its establishment or maintenance. However, no such role has been clearly demonstrated thus far in *Emx1* or *Emx2* single mutant mice, possibly due to functional redundancies between the two mouse genes (Yoshida *et al.*, 1997; Qiu *et al.*, 1996; Pellegrini *et al.*, 1996). In line with this possibility, the *Gli3* mutation, which abolishes the expression of both *Emx1* and *Emx2* in 10.0-dpc mouse embryos, results in morphological and molecular abnormalities at the demarcation between the dorsal diencephalon and the telencephalon (Theil *et al.*, 1999). Analyses of *Emx1* and *Emx2* double-mutant mice will be important to evaluate possible roles of *Emx* genes in the morphogenesis of this boundary.

***Dorsal diencephalon.*** While the *ScEmx3* expression domain is restricted to the dorsal telencephalon in 2.5-cm embryos, it initially spans more caudal territories. In an initial phase, *ScEmx3* expression pattern is dynamic, spanning a broad dorsal territory with posterior borders coincident with the prosencephalon/mesencephalon boundary when it becomes visible, and later spanning the dorsal telencephalon and anterior-most parts of the dorsal diencephalon. This early phase of expression, which is first detected at the onset of neurulation, is not observed for the paralogous genes *ScEmx1* and *ScEmx2* and has not been described in the lamprey thus far. In contrast, in the mouse as well as in the chick, *Emx2* (but not *Emx1*) is first transcribed at early neurula stages, in a broad dorsal territory initially showing a caudal border at the prosencephalon/mesencephalon limit and later regressing inside the diencephalon (Simeone *et al.*, 1992; Bell *et al.*, 2001). Similarly, in its earliest phase of expression, from early to midneurula stages, the *Xenopus XlEmx2* gene is transcribed in a broad dorsal domain of the forebrain, comprising both telencephalic and diencephalic presumptive territories, while *XlEmx1* transcription appears restricted to presumptive telencephalic territories (Pannese *et al.*, 1998). Identical conclusions have been suggested in the zebrafish, although the boundaries of *ZfEmx1* and *ZfEmx2* expression domains were not precisely mapped in this species (Morita *et al.*, 1995). These data suggest that an early *Emx* activity in the dorsal prosencephalon, including presumptive diencephalic territories, may be highly conserved among gnathostomes, suggesting an essential role in the specification of these territories. Despite this conservation, analyses of $Emx1^{-/-}$ or $Emx2^{-/-}$ mutant mice have failed to reveal such a role. However, studies of $Emx2^{-/-}/Otx2^{+/-}$ embryos have recently shown that *Emx2* and *Otx2* act cooperatively to specify dorsal diencephalic territories at early stages of the neural plate development (Suda *et al.*, 2001). Such a cooperative interaction between *Emx* and *Otx2* genes may be conserved in chondrichthyans, since in the dogfish as in osteichthyans, *Otx2* is

transcribed in the prospective prosencephalon and mesencephalon starting from the end of gastrulation (Mazan *et al.*, 2000 and data not shown). In this hypothesis, this interaction which involves Emx2 in sarcopterygians, clearly involves Emx3, a member of another orthology class, in the dogfish.

***Ventral diencephalon.*** In the dogfish, *ScEmx2*, but no other paralogue, shows a strong expression in the ventral diencephalon at the end of neurulation, which becomes restricted to the infundibulum when it becomes morphologically visible. A very similar *Emx2* expression has been described in the mouse, with a prominent expression in posterior parts of the ventral diencephalon starting from 9.5 dpc (Simeone *et al.*, 1992a,b) and in the posterior hypophysis at later stages (13.5 dpc). *Emx2* expressions in the ventral diencephalon have also been reported in the chick (stage HH12–HH13; Bell *et al.*, 2001), *Xenopus* (stage 37; Pannese *et al.*, 1998)m and zebrafish (24 h of development; Morita *et al.*, 1995). These data suggest that an *Emx2* expression in the ventral diencephalon may be highly conserved in gnathostomes. However, the biological significance of this conservation remains unclear, since the derivatives of the ventral diencephalon display no obvious defect either in $Emx2^{-/-}$ or $Emx2^{-/-}/Otx2^{+/-}$ embryos.

***Conclusion.*** Taken together, our data indicate that not only telencephalic, but also diencephalic *Emx* expression sites are highly conserved among gnathostomes at early stages of brain development. This conservation may seem paradoxical since relatively subtle defects have been thus far observed in mice carrying either $Emx1^{-/-}$ or $Emx2^{-/-}$ mutations. However, as suggested by analyses of *Gli3* or $Emx2^{-/-}/Otx2^{+/-}$ mutations, it could reflect a selective pressure for the maintenance of functional redundancies between the paralogous genes and possibly other homeodomain genes. An alternative, although not exclusive interpretation may be that some abnormalities may escape detection in laboratory conditions and provide a selective advantage at the population level (Cooke *et al.*, 1997). This may be particularly true for *Emx* genes, which in mammals, are involved in the arealization of the cortex (Bishop *et al.*, 2000; Mallamaci *et al.*, 2000) and in the morphogenesis of the hippocampus, a brain structure known to play an important role in memory processes (Pellegrini *et al.*, 1996; Yoshida *et al.*, 1997; Tole *et al.*, 2000).

### *ScEmx2 Expression in the Mesoderm Suggests a Role in the Segmentation of the Cephalic Mesoderm*

At the trunk level, the segmentation of the vertebrate paraxial mesoderm into somites has been extensively documented, and the underlying genetic and cellular mechanisms largely elucidated (reviewed in Pourquié, 2001). In contrast, the vertebrate cranial paraxial mesoderm, located anterior to the segmental plate, never condenses into somites and its organization has remained a matter of controversy for more than a century. Classic interpretations have proposed that it may consist of several segmental units, corresponding to vestigial forms of genuine segments present in a vertebrate ancestor (reviewed in Kuratani *et al.*, 1999; Holland, 2000). These segmental theories were largely influenced by morphological analyses of amphioxus embryos, which display a fully segmented organization of the paraxial mesoderm along the whole body length, including its most rostral aspects, but also of shark embryos, which exhibit three to four pairs of tandemly arranged cavities in the cephalic paraxial mesoderm. Different kinds of experimental evidence supporting these views have been more recently obtained. First, a strong support for a homology between the segmented anterior-most paraxial mesoderm present in amphioxus embryos, and the cephalic paraxial mesoderm lying rostral to rhombomere 5 in vertebrates, has emerged from comparative analyses of *Hox* expression patterns in these species (Holland, 2000). Second, a transient segmental pattern has been described in the cephalic paraxial mesoderm of a wide range of vertebrates, on the basis of scanning electron microscopy observations. Four tandemly arranged units, corresponding, from rostral to caudal levels, to the premandibular mesoderm, the mandibular mesoderm, the hyoid mesoderm, and the so-called somite 0 (a somite-like unit showing an incomplete segmental cleft at its anterior border), have thus been described at neural plate stages in lampreys, sharks, and amphibians (Kuratani *et al.*, 1999; Kuratani and Horigome, 2000; Jacobson and Meier, 1984). An early subdivision of the cephalic paraxial mesoderm in seven somitomeres has also been reported in amniotes as well as in teleosts, suggesting that modifications of an ancestral segmentation pattern may have independently occurred in these two groups (reviewed in Jacobson, 1988). Finally, a regionalization of the cephalic paraxial mesoderm has been unambiguously shown by cell lineage analyses in mouse and in chick embryos (Couly *et al.*, 1992; Trainor *et al.*, 1994). In the head region, the fate of paraxial mesoderm cells is predominantly myogenic but clearly differs along the rostrocaudal axis, cells located at prosencephalon and mesencephalon levels contributing to different oculomotor muscles, while those located at the rhombencephalon level colonize jaw muscles. However, in the absence of morphological landmarks, it is difficult to formally assign these different structures to individual segments. Furthermore, no genetic evidence supporting an early segmental pattern of the cephalic paraxial mesoderm has been obtained thus far, and the genetic mechanisms, which control its regionalization, remain completely unknown.

In this context, the highly spatially restricted mesoderm expression of *ScEmx2* strongly suggests its involvement in the early specification of a well-individualized component of the cephalic paraxial mesoderm, thus providing a strong genetic argument in favor of its segmental organization in the dogfish. This component most likely corresponds to the presumptive mandibular mesoderm, since the labeling appears restricted to cells that delimit the mandibular cavity when it becomes visible. Whether this *Emx* expression corresponds to a derived feature of sharks or a primitive

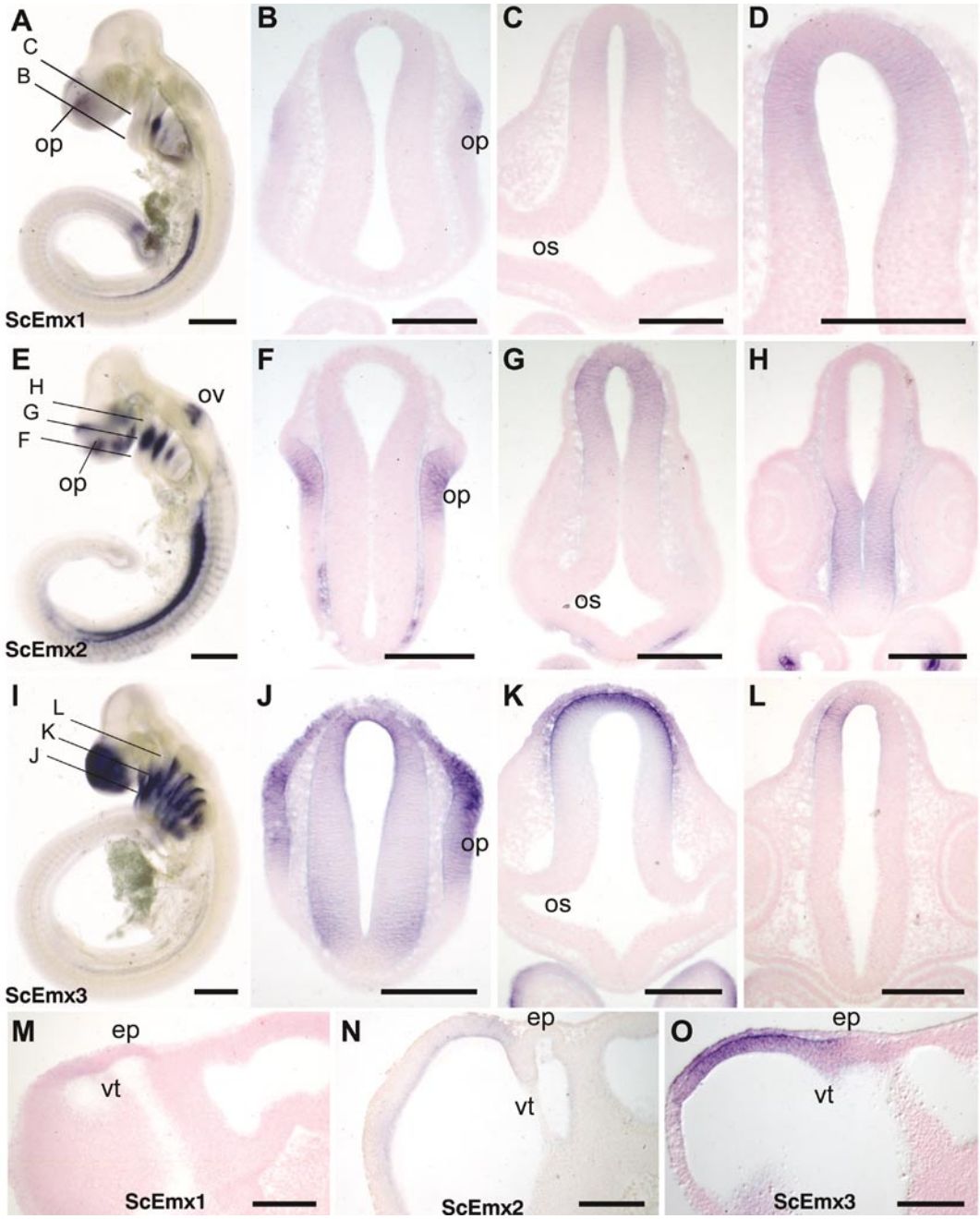


**FIG. 7.** Expression of *ScEmx1*, *ScEmx2*, and *ScEmx3* in the forebrain of stage 21–22 *S. canicula* embryos. (A, E, I) Lateral views of embryos after whole-mount hybridization using *ScEmx1*, *ScEmx2*, and *ScEmx3* antisense RNA probes, respectively. (A, E) Stage 21. (I) Stage 22. (B, C), (F–H), and (J–L) Transverse sections of the embryos shown in (A), (E), and (I), respectively. (D) Higher magnification of (C). The planes of sections are indicated by thin lines in (A), (E), and (I). (M, N, O) Sagittal sections of stage 21 (M, O) or stage 22 (N) embryos after whole-mount hybridization using *ScEmx1*, *ScEmx2*, and *ScEmx3* antisense RNA probes, respectively. ep, epiphysis primordium; op, olfactory placode; os, optic stalk; ov, otic vesicle; vt, velum transverse.

character of gnathostomes or even vertebrates, is an important, but unresolved issue. Thus far, no *Emx* expression in the paraxial mesoderm has been described either in osteichthyans, or in protochordates. In contrast, the *LjEmx* gene isolated in *L. japonica* shares an early mesodermal expression with *ScEmx2*, suggesting that this expression feature

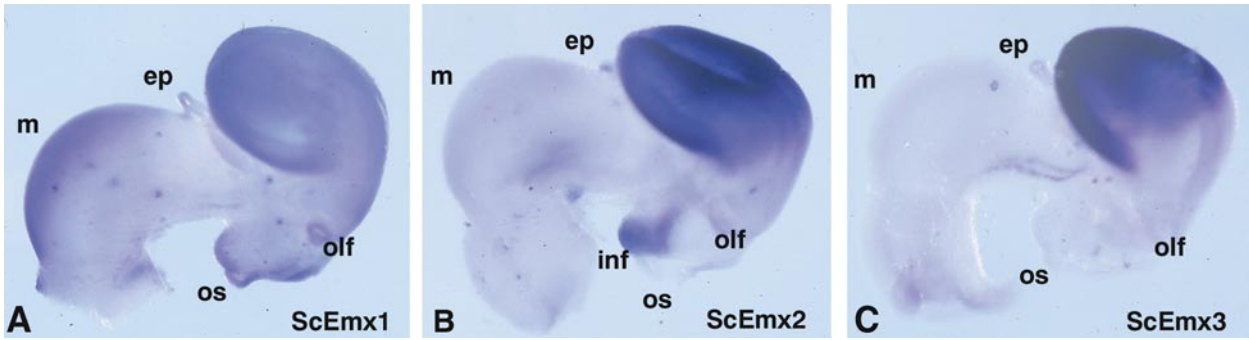


**FIG. 8.** Expression of *ScEmx1*, *ScEmx2*, and *ScEmx3* in the forebrain of 2.5-cm *S. canicula* embryos. (A–C) Lateral views of dissected brains after whole-mount hybridization using *ScEmx1*, *ScEmx2*, and *ScEmx3* antisense RNA probes, respectively. Same abbreviations as in Fig. 7; inf, infundibulum; m, mesoderm; olf, olfactory stalk.

may correspond to a vertebrate primitive character, lost in osteichthyans. However, in the lamprey, *LjEmx* expression is not restricted to cephalic regions, but spans the whole paraxial mesoderm (Myojin *et al.*, 2001). In this case, a posterior prevalence mechanism, involving a phenotypic suppression by *Hox* genes, such as the one described in *Drosophila*, could restrict the *Emx* activity to anterior-most regions (Macías and Morata, 1996). However, this remains a highly hypothetical scenario in view of the available data.

### *Conclusion: Functional Evolution of Emx Genes in Vertebrates*

It is currently widely accepted that massive gene duplications have occurred early in the vertebrate lineage, and previous analyses have led to the conclusion that *Emx* genes provide a novel example of these genetic events (Williams and Holland, 2000). Our analysis supports this conclusion since we show here that the duplication of *Emx* genes has predated the splitting of chondrichthyans and osteichthyans, which is consistent with the chronologies inferred from other genetic systems (Holland *et al.*, 1994).

Whether the diverse sites of expression shown by gnathostome *Emx* genes are primitive among chordates remains an opened question. The posterior epidermis during neurulation, where no expression of osteichthyan or lamprey *Emx* genes has been described thus far, is actually the only expression site shared by the ascidian *Emx* gene, one of the dogfish gene (*Emx3*), and possibly *Drosophila ems* (Oda and Saiga, 2001). Its biological significance is unclear. However, comparisons of the expression patterns displayed by the three dogfish paralogous genes and their osteichthyan counterparts provide insights into those already present in the ancestral *Emx* gene, which was duplicated in the vertebrate lineage to generate the three extant *Emx1*, *Emx2*, and *Emx3* orthology classes. Our data suggest that this ancestral gene already showed a complex expression pattern, including the dorsal prosencephalon during neurulation, an expression site shared by the dogfish *Emx3* and the tetrapod *Emx2* genes, the dorsal telencephalon during early organogenesis, where *LjEmx* and all gnathostome *Emx* genes are transcribed, but also the olfactory placodes, a site of *ScEmx2* and *ScEmx3* expression (only *Emx2* in tetrapods), and the urogenital system, a site of *ScEmx1*, *ScEmx2*, and *ScEmx3* expression (*Emx2* in the mouse). These sites of expression have subsequently been retained by different paralogs in different taxa, as proposed in the duplication–degeneration–complementation model of multigene family evolution (Force *et al.*, 1999). As a consequence, gnathostome *Emx* genes provide a novel example of "shuffling" of expression domains, and possibly function, between paralogues, such as those observed between the zebrafish *Hoxa-1* and the mouse *Hoxb-1* genes (McClintock *et al.*, 2001), or the mouse and chick *slug* and *snail* genes (Sefton *et al.*, 1998). This does not preclude possible functionalizations of one orthology class for other *Emx* functions. For instance, in the dogfish as in osteichthyans, *Emx2*, but no other paralog, is expressed in the otic vesicle and the ventral diencephalon during neurulation. The identification of residues, which are selectively conserved in each orthology class, also suggests that different structural constraints may act on Emx1, Emx2, and Emx3 proteins. In this respect, it is noticeable that a number of Emx2-specific residues are located in the immediate proximity of a protein motif also conserved in *Drosophila* ems (FYPW). In Hox proteins, a related protein sequence (YPWM), similarly located at a short distance upstream the homeodomain, is known to be an important component of protein–protein interactions which increase the specificity and affinity of Hox–DNA binding (Passner *et al.*, 1999). Taken together, these data support the idea that the three paralogous proteins may be involved in different protein–protein interactions, whose affinity and specificity could be modulated by the residues selectively conserved in each class. Combinations of functional and comparative approaches will be necessary to gain further insights into the molecular mechanisms underlying the diversification of *Emx* genes in gnathostomes.

## ACKNOWLEDGMENTS

The *F. rubripes* sequences were provided freely by the Fugu Genome Consortium for use in this publication only. We thank N. Narradon for her help in typing the manuscript, and M. Pradels for her excellent technical assistance. We are grateful to M. and Mme. Le Maître and all the Pêcheries d'Armorique staff for their help in obtaining dogfish embryos. This work was supported by grants from the Centre National de la Recherche Scientifique, the Université Paris-Sud, the Fondation de la Recherche Médicale, and by fellowships from the Ministère de la Recherche et de la Technologie (to Y.D., T. S.-S., and J.-L.P.).

## REFERENCES

Adachi, J., and Hasegawa, M. (1996). MOLPHY version 2.3: Programs for molecular phylogenetics I PROTML: Maximum likelihood inference of protein phylogeny. *Comput. Sci. Monogr.* **28,** 1–150.

Altschul, S. F., Madden T. L., Schäffer, A. A., Zhang., J., Zhang, Z., Miller, W., and Lipman, D. J. (1997). Gapped BLAST and PSI-BLAST: A new generation of protein database search programs. *Nucleic Acids Res.* **25,** 3389–3402.

Arendt, D., and Nübler-Jung, K. (1996). Common ground plans in early brain development in mice and flies. *BioEssays* **18,** 255–259.

Arendt, D., and Nübler-Jung, K. (1999). Comparison of early nerve cord development in insects and vertebrates. *Development* **126,** 2309–2325.

Ballard, W. W., Mellinger, J., and Lechenault, H. A. (1993). A series of normal stages for development of *Scyliorhinus canicula*, the lesser spotted dogfish (Chondrichthyes: Scyliorhinidae). *J. Exp. Zool.* **267,** 318–336.

Bell, E., Ensini, M., Gulisano, M., and Lumsden, A. (2001). Dynamic domains of gene expression in the early avian forebrain. *Dev. Biol.* **236,** 76–88.

Bishop, K. M., Goudreau, G., and O'Leary, D. D. M. (2000). Regulation of area identity in the mammalian neocortex by *Emx2* and *Pax6*. *Science* **288,** 344–349.

Cooke, J., Nowak, M. A., Boerlijst, M., and Maynard-Smith, J. (1997). Evolutionary origins and maintenance of redundant gene expression during metazoan development. *Trends Genet.* **13,** 360–364.

Couly, G. F., Coltey, P. M., and Le Douarin, N. (1992). The developmental fate of the cephalic mesoderm in quail-chick chimeras. *Development* **114,** 1–5.

Force, A., Lynch, M., Pickett F. B., Amores, A., Yan, Y. L., and Postlethwait, J. (1999). Preservation of duplicate genes by complementary, degenerative mutations. *Genetics* **151,** 1531–1545.

Hirth, F., Therianos, S., Loop, T., Gehring, W. J., Reichert, H., and Furukubo-Tokunaga, K. (1995). Developmental defects in brain segmentation caused by mutations of the homeobox genes *orthodenticle and empty spiracles* in *Drosophila*. *Neuron* **15,** 769–778.

Hirth, F., and Reichert, H. (1999). Conserved genetic programs in insects and mammalian brain development. *BioEssays* **21,** 677–684.

Holland, P. W. H., Garcia-Fernandez, J., Williams, N. A., and Sidow, A. (1994). Gene duplications and the origins of vertebrate development. *Dev. Suppl.*, 125–133.

Holland, P. W. H. (2000). Embryonic development of heads, skeletons and amphioxus: Edwin S. Goodrich revisited. *Int. J. Dev. Biol.* **44**, 29–34.

Jacobson, A. G., and Meier, S. (1984). Morphogenesis of the head of a newt: mesodermal segments, neuromeres, and distribution of neural crest. *Dev. Biol.* **106,** 181–193.

Jacobson, A. G. (1988). Somitomeres: Mesodermal segments of vertebrate embryos. *Development* **104**(Suppl.), 209–220.

Kishino, H., Miyata, T., and Hasegawa, M. (1990). Maximum likelihood inference of protein phylogeny and the origin of chloroplasts. *J. Mol. Evol.* **30,** 151–160.

Kuratani, S., Horigome, N., and Hirano, S. (1999). Developmental morphology of the head mesoderm and reevaluation of segmental theories of the vertebrate head: Evidence from embryos of an agnathan vertebrate *Lampetra japonica*. *Dev. Biol.* **210,** 381–400.

Kuratani, S., and Horigome, N. (2000). Developmental morphology of branchiomeric nerves in a cat shark, *Scyliorhinus torazame*, with special reference to rhombomeres, cephalic mesoderm, and distribution patterns of cephalic crest cells. *Zool. Sci.* **17,** 893–909.

Macías, A., and Morata, G. (1996). Functional hierarchy and phenotypic suppression among *Drosophila* homeotic genes: The *labial* and *empty spiracles* genes. *EMBO J.* **2,** 334–343.

Mallamaci, A., Muzio, L., Chan, C-H., Parnavelas, J., and Boncinelli, E. (2000). Area identity shifts in the early cerebral cortex of $Emx2^{-/-}$ mutant mice. *Nat. Neurosci.* **3,** 679–686.

Mazan, S., Jaillard, D., Baratte, B., and Janvier, P. (2000). Otx1 gene-controlled morphogenesis of the horizontal semicircular canal and the origin of the gnathostome characteristics. *Evol. Dev.* **2,** 186–193.

McClintock, J. M., Carlson, R., Mann, D. M., and Prince, V. E. (2001). Consequences of Hox gene duplication in the vertebrates: An investigation of the zebrafish Hox paralogue group 1 genes. *Development* **128,** 2471–2484.

Miyamoto, N., Yoshida, M., Kuratani, S., Matsuo, I., and Aizawa, S. (1997). Defects of urogenital development in mice lacking *Emx2*. *Development* **124,** 1653–1664.

Miyoko, M., Ueki, T., Sugahara, F., Murakami, Y., Shigetani, Y., Aizawa, S., Hirano, S., and Kuratani, S. (2001). Isolation of *Dlx* and *Emx* genes cognates in an agnathan species, *Lampetra japonica*, and their expression patterns during embryonic and larval development: Conserved and diversified regulatory patterns of homeobox genes in vertebrates head evolution. *J. Exp. Zool.* **291,** 68–84.

Morita, T., Nitta, H., Kiyama, Y., Mori, H., and Mishina, M. (1995). Differential expression of two zebrafish *emx* homeoprotein mRNas in the developing brain. *Neurosci. Lett.* **198,** 131–134.

Murakami, Y., Ogasawara, M., Sugahara, F., Hirano, S., Satoh, N., and Kuratani, S. (2001). Identification and expression of the lamprey *Pax6* gene: Evolutionary origin of the segmented brain of vertebrates. *Development* **128,** 3521–3531.

Myojin, M., Ueki, T., Sugahara, F., Murakami, Y., Shigetani, Y., Aizawa, S., Hirano, S., and Kuratani, S. (2001) Isolation of *Dlx*, and *Emx*. gene cognates in an agnathan species, *Lampetra japonica*, and their expression patterns during embryonic and larval development: conserved and diversified regulatory patterns of homeobox genes in vertebrate head evolution. *J. Exp. Zool.* **291,** 68–84.

Oda, I., and Saiga, H. (2001). *Hremx*, the ascidian homologue of *ems/emx*, is expressed in the anterior and posterior-lateral epidermis but not in the central nervous system during embryogenesis. *Dev. Genes Evol.* **211,** 291–298.

Pannese, M., Lupo, G., Kablar, B., Boncinelli, E., Barsacchi, G., and Vignali, R. (1998). The *Xenopus Emx* genes identify presumptive dorsal telencephalon and are induced by head organizer signals. *Mech. Dev.* **73,** 73–83.

Passner, J. M., Ryoo, H. D., Shen, L., Mann, R. S., and Aggarwal, A. (1999). Structure of a DNA-bound Ultrabithorax–Extradenticle homeodomain complex. *Nature* **397,** 714–719.

Patarnello, T., Bargelloni, L., Boncinelli, E., Spada, F., Pannese, M., and Broccoli, V. (1997). Evolution of *Emx* genes and brain development in vertebrates. *Proc. R. Soc. Lond. B. Biol. Sci.* **264,** 1763–1766.

Pellegrini, M., Mansouri, A., Simeone, A., Boncinelli, E., and Gruss, P. (1996). Dentate gyrus formation requires *Emx2*. *Development* **122,** 3893–3898.

Pellegrini, M., Pantano, S., Lucchini, F., Fumi, M., and Forabosco, A. (1997). *Emx2* developmental expression in the primordia of the reproductive and excretory systems. *Anat. Embryol.* **196,** 427–433.

Pourquié, O. (2001). Vertebrate somitogenesis. *Annu. Rev. Cell Dev. Biol.* **17,** 311–350.

Philippe, H. (1993). MUST, a computer package of Management Utilities for Sequences and Trees. *Nucleic Acids Res.* **21,** 5264–5272.

Qiu, M., Anderson, S., Chen, S., Meneses, J. J., Hevner, R., Kuwana, E., Pedersen, R. A., and Rubenstein, J. L. R. (1996). Mutation of the *Emx-1* homeobox gene disrupts the corpus callosum. *Dev. Biol.* **178,** 174–178.

Rzhetsky, A., and Nei, M. (1994). Unbiased estimates of the number of nucleotide substitutions when substitution rate varies among different sites. *J. Mol. Evol.* **38,** 295–299.

Saitou, N., and Nei, M. (1987). The neighbor-joining method: A new method for reconstructing phylogenetic trees. *Mol. Biol. Evol.* **4,** 406–425.

Sefton, M., Sanchez, S., and Nieto, M. A. (1998). Conserved and divergent roles for members of the Snail family of transcription factors in the chick and mouse embryos. *Development* **125,** 3111–3121.

Simeone, A., Gulisano, M., Acampora, D., Stornaiuolo, A., Rambaldi, M., and Boncinelli, E. (1992a). Nested expression domains of four homeobox genes in developing rostral brain. *Nature* **358,** 687–690.

Simeone, A., Gulisano, M., Acampora, D., Stornaiuolo, A., Rambaldi, M., and Boncinelli, E. (1992b). Two vertebrate homeobox genes related to the *Drosophila empty spiracles* gene are expressed in the embryonic cerebral cortex. *EMBO J.* **11,** 2541–2550.

Suda, Y., Hossain, Z. M., Kobayashi, C., Hatano, O., Yosida, M., Matsuo, I., and Aizawa, S. (2001). *Emx2* directs the development of diencephalon in cooperation with *Otx2*. *Development* **128,** 2433–2450.

Swofford, D. L. (1993). PAUP: Phylogenetic Analysis Using Parsimony, version 3.1.1. Computer program distributed by the Illinois Natural History Survey, Champaign, Illinois.

Theil, T., Alvarez-Bolado, G., Walter, A., and Rüther, U. (1999). *Gli3* required for *Emx* gene expression during dorsal telencephalon development. *Development* **126,** 3561–3571.

Trainor, P. A., Tan, S-S., and Tam, P. P. L. (1994). Cranial paraxial mesoderm: regionalisation of cell fate and impact on craniofacial development in mouse embryos. *Development* **120,** 2397–2408.

Tole, S., Goudreau, G., Assimacopoulos, S., and Grove, E. A. (2000). *Emx2* is required for growth of the hippocampus but not for hippocampal field specification. *J. Neurosci.* **20,** 2618–2625.

Yoshida, M., Suda, Y., Matsuo, I., Miyamoto, N., Takeda, N., Kuratani, S., and Aizawa, S. (1997). *Emx1* and *Emx2* functions in development of dorsal telencephalon. *Development* **124,** 101–111.

Williams, N. A., and Holland, P. W. H. (2000). An amphioxus *Emx* homeobox gene reveals duplication during vertebrate evolution. *Mol. Biol. Evol.* **17,** 1520–1528.

Xu, Q., and Wilkinson, D. J. (1993). In "In Situ Hybridization: A Practical Approach" (D. G. Wilkinson, Ed.), pp. 69–86. Oxford Univ. Press, Oxford.

Received for publication March 7, 2002
Revised April 16, 2002
Accepted April 17, 2002
Published online June 7, 2002